ing, one of the most fundamental questions associated with crack dynamics is the maximum speed that cracks can propagate. Depending on the type of loading (e.g., tensile, shear, or antiplane shear), there is a unique maximum speed cracks can achieve. For tensile-loaded cracks, theory predicts that this limiting speed is the Rayleigh wave speed, the speed of elastic waves on a surface. Recent theoretical work, including atomistic simulations, has challenged this classical view. Now, P.J. Petersan and co-workers from the University of Texas at Austin have shown experimentally that tensile-loaded cracks in rubber can actually propagate faster than the Rayleigh wave speed and even break the sound barrier.

As reported in the July issue of *Physical Review Letters* (105504), Petersan and colleagues identified the intersonic crack speed by the observation of shock fronts near the crack tip by high-speed photography (see Figure 1). The experiments were conducted using highly stretched sheets of rubber. In this nonlinear material, cracks in tension (mode I) exceeded the shear wave speed and traveled in the intersonic range between shear and longitudinal wave speeds. These results have important implications for understanding fundamental crack dynamics, demonstrating that the classical understanding of crack dynamics needs to be revised.

What is the physical explanation for this phenomenon? Through observations made earlier in large-scale molecular dynamics simulations, M.J. Buehler and H. Gao of Max Planck Institute, Stuttgart, and F.F. Abraham of Almaden Research Center in San Jose discovered that hyperelasticity (i.e., the elasticity of materials at large strains), although mostly neglected in existing theories of fracture, is crucial in understanding crack dynamics. In their article published in the November 13, 2003, issue of *Nature* (p. 141), Buehler and colleagues hypothesized that energy flow toward a crack tip occurs in a region whose size is described by a so-called characteristic energy length scale χ. This length scale competes with the size of the hyperelastic region. If the size of the region of energy flow χ is comparable to the size of the hyperelastic region (r_H), energy flow is completely dominated by the local large-strain or hyperelastic properties.

"For instance," Buehler said, "if material stiffens with strain as in the case of rubber used in Petersan's experiments and in the molecular dynamics simulations, energy flow is enhanced because of the stiffer material properties, and cracks can thus break through the sound barrier. The observation of intersonic mode I cracks in rubber seems to be an example for the importance of hyperelastic effects in real materials."

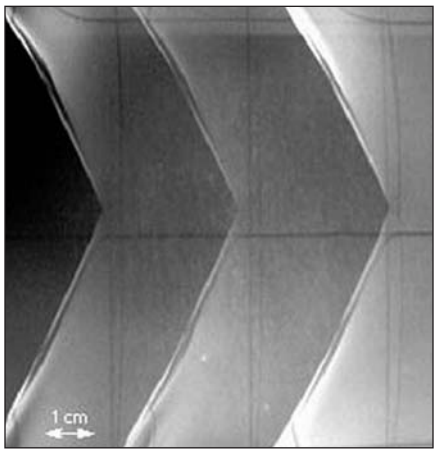

Figure 1. Multiple-exposure photograph of a crack propagating in a rubber sample (λ_x = 1.2, λ_y = 2.4); speed of the crack, ~56 m/s.

Petersan said, "We agree that the rupture of rubber opens up a new regime in the study of fracture and look forward to understanding the mechanism which explains it."

Fluorine-Containing Molecules Serve as Structure-Directing Agents in Synthesis of Molecular Sieves

Water-soluble organic molecules have been used as structure-directing agents (SDAs) in the synthesis of zeolites. By filling the cavities in the material, these molecules direct the hydrothermal crystallization of zeolite and zeolite-like materials. Usually, hydrogen atoms attached to the organic molecules are in charge of the chemical interaction with the zeolite inorganic framework. By replacing hydrogen atoms with fluorine atoms as SDAs, J. Pérez-Pariente and colleagues at the Instituto de Catálisis y Petroleoquímica, Spain, significantly changed the surface properties of their zeolites.

As reported in the August 24 issue of *Chemistry of Materials* (p. 3209), the researchers prepared a group of fluorine-containing SDAs such as 1-(fluorobenzyl)-pyrrolidine (F-PB) and difluorinated dibenzyldimethyl-ammonium cations (DBDM) by reacting *o*-, *m*-, or *p*-fluorobenzyl chloride with pyrrolidine, dimethylamine, or benzyldimethylamine. Inorganic gels and SDAs (1:1:1:*x*:40 $R:Al_2O_3:P_2O_5:SiO_2:H_2O$, where R is the SDA and *x* is 0 for alumino-phosphate, AlPO, and 0.5 for silico-alumino-phosphate, SAPO, gels) were heated at 150ºC for 72 h. Another silica gel (0.54:0.54:1:7.93 $R:HF:SiO_2:H_2O$) with the quaternary monofluorinated DBDM cations was heated at 135ºC for 46 days in a fluoride medium. The control material AlPO-5 (AFI), which is an aluminophosphate with 12MR (12-membered ring) one-dimensional channels, was made from benzylpyrrolidine (BP).

X-ray diffraction patterns of the different materials revealed that the nature and crystallinity of the monofluorinated derivatives used as SDAs depended strongly on the position of the fluorine atom in the aromatic ring. The crystallinity of the materials was found to be higher when fluorine was in the *meta*-fluoro (mF) position rather than in the *para*-fluoro (pF) position, and the stability of the AlPO-5 crystal (framework code type AFI) structure with different SDAs follows the order mF-BP > BP > oF[*ortho*]-BP >> pF-BP. The researchers said that the *meta*-fluoro derivative served as the best template because of the electrostatic interactions between the fluorine atom and the inorganic zeolite pore; the *ortho*- and *para*-fluoro derivatives showed poor crystallinity of the AFI phase in the product due to the structural hindrance. Magic angle spinning nuclear magnetic resonance data showed that the template molecules were intact inside both zeolites (DBDM), which were made in a fluoride medium, and AFI(BP) materials.

LUCY YUE HU

Flame-Spraying Technique Yields Aluminate Bulk Glasses and Nanoceramics

Alumina, Al_2O_3, is the basis of a number of important ceramic systems. It is desirable to form alumina-rich bulk glasses because of their superior mechanical, chemical, and optical properties. However, it is very difficult to form bulk glass from pure alumina liquid, a reluctant glass former, because of the extremely high cooling rates required, typically in the range of 10^7 K s^{-1}. The addition of rare-earth oxides reduces the cooling rates to under 10^3 K s^{-1}, which is still too high to obtain glasses with dimensions of more than a few millimeters. A. Rosenflanz and co-workers at 3M in Minnesota have utilized a flame-spraying technique to generate glass beads that contain 80 mol% alumina (the balance is rare-earth oxide). They then sintered the beads, yielding bulk alumina glass with the appropriate shape. Devitrification of the bulk glass using heat treatment resulted in a nanoceramic with twice the hardness of the original bulk glass.

As Rosenflanz and colleagues reported

https://doi.org/10.1557/mrs2004.199 Published online by Cambridge University Press

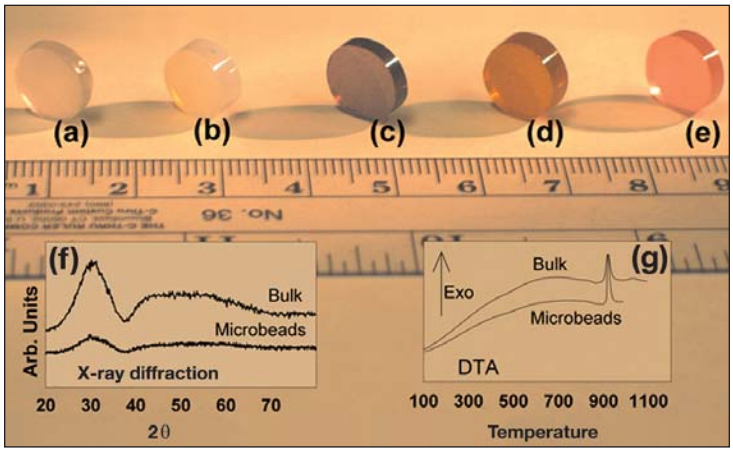

Figure 1. Bulk rare-earth aluminate glasses with the ALZ composition formed using the method described. No dopants were used for samples (a) and (b), while 5 wt% Nd_2O_3, Eu_2O_3, and Er_2O_3 were used for samples (c), (d), and e), respectively. Image (f) shows x-ray diffraction patterns, while (g) shows differential thermal analysis data for the microbead and bulk forms, revealing their amorphous nature and similar thermal behavior. Reprinted with permission from Nature ***430*** *(August 12, 2004) p. 762. ©2004 Nature Publishing Group.*

in the August 12 issue of *Nature* (p. 761), binary eutectic compositions of alumina and rare-earth oxide (Al_2O_3-RE_2O_3, RE = La, Gd, Y) as well as Al_2O_3:RE_2O_3:ZrO_2 (ALZ) ternary compositions were investigated. In their flame-spraying technique, particulate precursors were fed into a high-temperature hydrogen–oxygen flame, producing molten particles that were then quenched in water. Glassy beads of the material with diameters of less than 140 μm were obtained. Beads with diameters in the range of 75–109 μm (selected by sieving) were consolidated into bulk glasses by sintering the beads at a temperature within the kinetic window—between T_g (the glass-transition temperature) and T_x (the crystallization temperature). X-ray diffraction, differential thermal analysis, optical microscopy, and scanning electron microscopy revealed that the bulk glass that formed remained amorphous and transparent (see Figure 1).

The alumina-rich bulk glass was then heated above T_x for a short time to form a nanoscale glass–ceramic as a result of simultaneous crystallization and grain growth. The final microstructure contained ~100 nm crystalline grains, a finer and more homogeneous microstructure than that obtained using traditional methods. The glass–ceramics formed in this way also showed superior chemical, mechanical, and optical properties, as compared with silica-based glasses.

This technique yielded alumina-based glass–ceramic composites with superior fracture toughness, important for potential structural applications. This discovery of glass-forming ability and glass-converted nanoscale ceramics can be extended to other nonconventional bulk oxide systems as well, so long as a sufficiently wide kinetic window $\Delta T_x = T_x - T_g$ is available. The method could pave the path to numerous bulk oxide glasses and nanocrystalline ceramics.

GOPAL RAO

Composite Polymer–Carbon Nanotubes Function as Optoelectronic Memory Devices

In the past few years, interest in making nanoscale electronic devices from carbon nanotubes has skyrocketed, with the hopes of making devices that are smaller and more versatile. In the September issue of *Nano Letters* (p. 1587), A. Star from Nanomix Inc., G. Grüner from the University of California, Los Angeles, and co-workers report the fabrica-

https://doi.org/10.1557/mrs2004.199 Published online by Cambridge University Press